Journal of Zhejiang University SCIENCE A
ISSN 1673-565X (Print); ISSN 1862-1775 (Online)
www.zju.edu.cn/jzus; www.springerlink.com
E-mail: jzus@zju.edu.cn

Property of critical excitation for moment-resisting frames subjected to horizontal and vertical simultaneous ground motions*

Kohei FUJITA, Izuru TAKEWAKI†‡

(*Department of Urban and Environmental Engineering, Graduate School of Engineering, Kyoto University, Nishikyo-ku 615-8540, Japan*)

†E-mail: takewaki@archi.kyoto-u.ac.jp

Received July 7, 2009; Revision accepted July 27, 2009; Crosschecked July 29, 2009

Abstract: It has often been reported that, when building structures are subjected to near-fault earthquake ground motions, horizontal and vertical impulsive inputs may cause critical damage during the first few seconds. In practical design of building structures, however, the safety check, taking into account the effect of multi-component ground motions, is hardly conducted except the design of important structures such as high-rise buildings and nuclear power plants. Furthermore, it is not clear how the correlation of multi-component ground motions influences the actual safety of structures. In this paper, the detailed property of critical excitation is discussed in association with the relationship between the characteristics of ground motions and those of structures. The properties of various auto power spectral density (PSD) functions of the horizontal and vertical ground motions are investigated, and those of the critical cross PSD function of these two-directional ground motions are found by a devised algorithm in a feasible complex plane. A closed-form expression is derived from the critical relation of the auto PSD functions of the simultaneous inputs. This critical excitation method provides us with a new approach for earthquake-resistant design against the possible future earthquake which causes the critical damages to buildings.

Key words: Critical excitation, Multi-component ground input, Critical cross spectrum, Coherency, Simultaneous input
doi:10.1631/jzus.A0930002 **Document code:** A **CLC number:** P315

INTRODUCTION

After the Hyogoken-Nambu earthquake (1995), various discussions have been made on the possibility of occurrence and existence of impulsive and simultaneous inputs from horizontal and vertical directions to building structures (e.g., Japanese Geotechnical Society, 1996). This kind of great earthquake ground motions occurs in the long return period (Strasser and Bommer, 2009), and it may be difficult to investigate the actual recorded ground motions of large intensity and with various properties.

To overcome this difficulty, several critical excitation approaches have been proposed and various useful methods have been provided (Drenick, 1970; Iyengar and Manohar, 1987; Manohar and Sarkar, 1995; Sarkar and Manohar, 1996; Takewaki, 2001; 2002; 2004a; 2004b; 2006a; 2006b; Abbas and Manohar, 2002a; 2002b; 2007; Abbas and Takewaki, 2009; Fujita *et al*., 2008a; 2008b). The work by Sarkar and Manohar (1996; 1998) and Abbas and Manohar (2002b) are concerned with the present paper although their papers deal with different models of multiple inputs at different points. Sarkar and Manohar (1996; 1998) formulated an interesting problem and solved the problem within the framework of limited variables. In particular, they treated only correlation in terms of 'the absolute value' of the cross power spectrum density (PSD) function (root-mean-square (RMS) of sum of the squares of co-spectrum and quad-spectrum). On the other hand, Abbas and Manohar (2002a) presented another interesting method including a detailed analysis of cross-correlation between multiple inputs at different points.

In most of the current structural design practice of building structures, safety and functionality checks

‡ Corresponding author

* Project supported by the Grant-in-Aid for Scientific Research of Japan Society for the Promotion of Science (Nos. 18360264 and 21360267)

are made with respect to one-directional earthquake input. It may also be understood that an approximate safety margin is incorporated in the magnitude of one-directional input. However, a more reliable method is desired (e.g., Smeby and Der Kiureghian (1985) for multi-component input). In this paper, horizontal and vertical simultaneous ground motions are treated and critical aspects of these ground motions are discussed in detail. The combinations of auto PSD functions of respective inputs are key parameters for discussion. A closed-form expression of the critical relation of the auto PSD functions of simultaneous inputs is derived with a detailed analysis of the critical relation.

ANALYSIS OF COHERENCE OF RECORDED BI-DIRECTIONAL GROUND MOTIONS

In this paper, the coherence function is assumed to be fixed at 1.0. This assumption means that horizontal and vertical ground motions are fully correlated, but it is not commonly known what degree of correlation the multi-component ground motions have. For this reason, it is meaningful to investigate the correlation between recorded bi-directional ground motions.

Fig.1(a-1) shows the representative acceleration records of El Centro north-south (NS) and up-down (UD) (Imperial Valley earthquake, 1940), Fig.1(b-1) those of NIG018 NS and UD (Niigataken Chuetsu-oki earthquake, 2007), and Fig.1(c-1) those of Japan Meteorological Agency (JMA) Kobe NS and UD (Hyogoken-Nambu Imperial Valley earthquake, 1995). Table 1 indicates the area (power) of the auto PSD function of these ground motions. For these data, Figs.2a~2c indicate the distribution of coherence functions for three time intervals. The auto PSD functions and cross PSD functions have been calculated from the Fourier transforms by using the Welch-Bartlett method. As shown in Figs.1(a-2), 1(b-2), and 1(c-2), the starting time of the window with the duration T (5 s in El Centro, NIG018 and JMA Kobe) was changed successively (time-lag of 0.02 s for El Centro and JMA Kobe and 0.01 s for NIG018) and the corresponding set of data for the 50 windows was chosen to represent candidates of the ensemble mean. Then the ensemble mean was taken of the functions computed from the Fourier transforms. It can be observed that the coherence strongly depends on the type of earthquake ground motions. Furthermore, it has been investigated that the coherence also depends on the portion of ground motions. The prediction of the coherence function before its occurrence is quite difficult and the critical excitation method will provide a meaningful insight even in these circumstances.

Table 1 Area of auto power spectral density (PSD) function for recorded ground motion

Recorded ground motion	Power (m^2·rad/s^4)	
	Horizontal	Vertical
El Centro NS, UD (1940)	1.478	0.365
NIG018 NS, UD (2007)	8.878	2.253
JMA Kobe NS, UD (1995)	8.001	1.733

MODELING OF HORIZONTAL AND VERTICAL STOCHASTIC GROUND MOTIONS

It is assumed here that horizontal and vertical simultaneous ground motions (HVGMs) can be described by the following uniformly modulated non-stationary model:

$$\ddot{u}_g(t) = c_u(t) w_u(t), \tag{1}$$

$$\ddot{v}_g(t) = c_v(t) w_v(t), \tag{2}$$

where $c_u(t)$, $c_v(t)$ are the envelope functions and $w_u(t)$, $w_v(t)$ are the stationary random processes (zero-mean Gaussian). The time-lag between the horizontal and vertical ground motions can be expressed in terms of $c_u(t)$, $c_v(t)$.

The envelope function $c_u(t)$ is given by

$$\begin{aligned} c_u(t) &= (t/3.0)^2, && (0 \le t \le 3), \\ c_u(t) &= 1.0, && (3 \le t \le 12.5), \\ c_u(t) &= \mathrm{e}^{-0.24(t-12.5)}, && (12.5 \le t \le 40). \end{aligned} \tag{3}$$

The envelope function $c_v(t)$ can also be given by Eq.(3). Fig.3a shows an example of the envelope function.

The stationary random processes (zero-mean Gaussian) $w_u(t)$, $w_v(t)$ can be generated from the auto PSD functions, and the multi-component ground motion can then be generated by the multiplication of these functions with the corresponding envelope functions (Fig.3b).

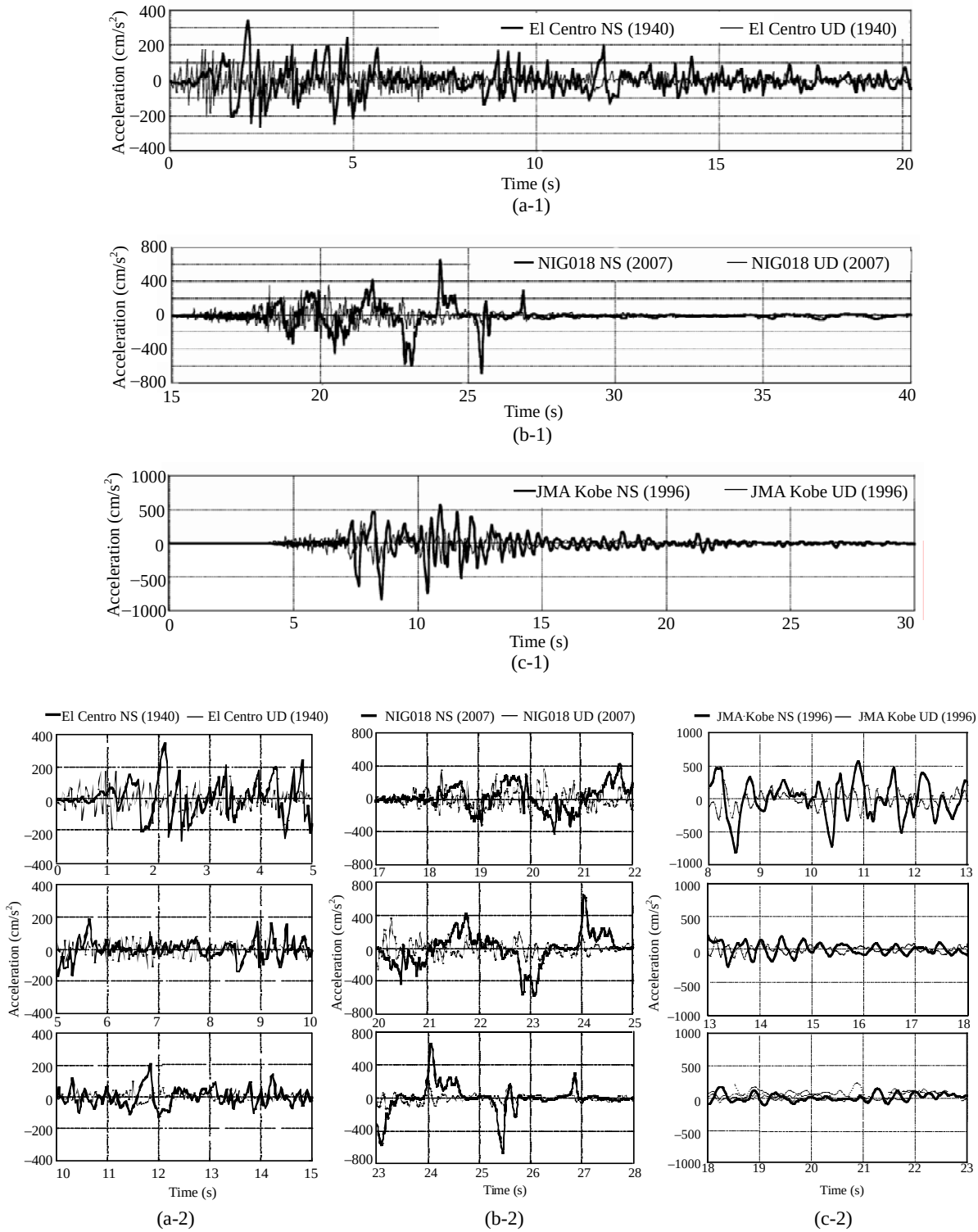

Fig.1 Acceleration records of (a-1) El Centro 1940 NS and UD (Imperial Valley earthquake); (b-1) NIG018 2007 NS and UD (Niigata-Ken Chuuetsu Oki earthquake); (c-1) JMA Kobe 1995 NS and UD (Hyogo-Ken Nambu earthquake). (a-2), (b-2) and (c-2) are enlarged images of (a-1), (b-1) and (c-1), respectively

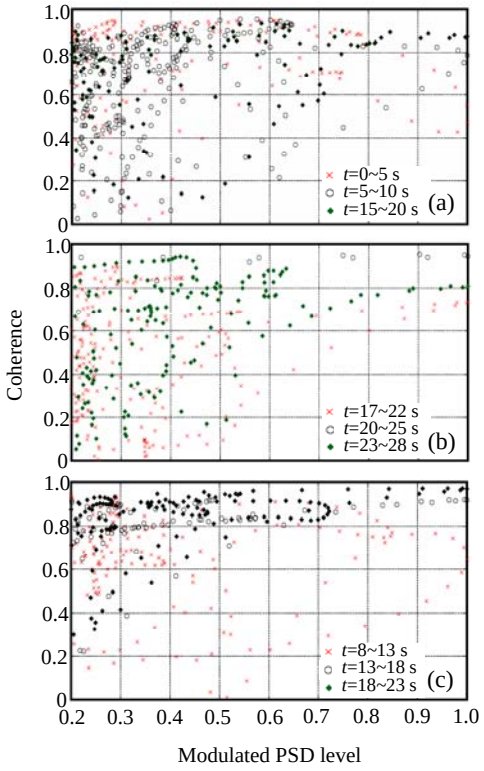

Fig.2 Coherence functions of recorded accelerations. (a) El Centro 1940 NS and UD (Imperial Valley earthquake); (b) NIG018 2007 NS and UD (Niigata-Ken Chuuetsu Oki earthquake); (c) JMA Kobe 1995 NS and UD (Hyogo-Ken Nambu earthquake)

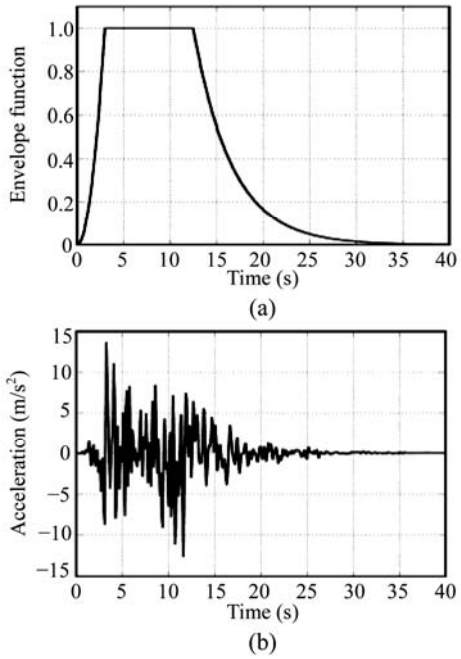

Fig.3 (a) Envelope function; (b) Example of non-stationary ground motion

STRUCTURAL MODEL SUBJECTED TO HORIZONTAL AND VERTICAL SIMULTANEOUS GROUND INPUTS

Consider a moment-resisting frame subjected to HVGM. The columns have a square-tube cross section and the beam has a wide-flange cross section as shown in Fig.4. The storey height is H and the span length of the frame is L. Let E, I_b and I_c denote the Young's modulus of the beam and columns, the second moment of area of beam and column, respectively.

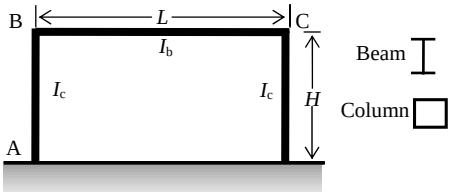

Fig.4 One-storey one-span plane frame consisting of beam of wide-flange cross-section and column of square-tube cross-section

Assume that the vibration in each direction of the moment-resisting frame can be expressed by the single-degree-of-freedom (SDOF) model. The equivalent horizontal and vertical stiffnesses k_u, k_v of the SDOF model are expressed respectively by Fujita *et al*.(2008a)

$$k_u=\frac{12EI_c[1+6(I_b/I_c)(H/L)]}{H^3[2+3(I_b/I_c)(H/L)]}, \tag{4}$$

$$k_v=\frac{96EI_b[2+(I_b/I_c)(H/L)]}{L^3[1+2(I_b/I_c)(H/L)]}. \tag{5}$$

The bending moments at the beam-end under the respective input of HVGM may be expressed as

$$M_u(t)=\frac{18EI_b}{HL\{2+3(I_b/I_c)(H/L)\}}u(t)\equiv A_{M_u}u(t), \tag{6}$$

$$M_v(t)=\frac{24EI_b}{L^2\{1+2(I_b/I_c)(H/L)\}}v(t)\equiv A_{M_v}v(t), \tag{7}$$

where $u(t)$ is the horizontal displacement of node B (Fig.4) and $v(t)$ is the vertical displacement of the central point of floor.

Let $\omega_u=\sqrt{k_u/m_u}$, $\omega_v=\sqrt{k_v/m_v}$ denote the fundamental natural circular frequencies in the horizontal and vertical vibrations, respectively, of the SDOF model. The horizontal and vertical displacements of the floor can be derived as

$$u(t)=\int_0^t\left\{-\ddot{u}_g(\tau)\right\}g_u(t-\tau)\mathrm{d}\tau, \tag{8}$$

$$v(t)=\int_0^t\left\{-\ddot{v}_g(\tau)\right\}g_v(t-\tau)\mathrm{d}\tau, \tag{9}$$

where $g_u(t)$, $g_v(t)$ are unit impulse response functions.

By using Eqs.(6)~(9), $M_u(t)$ and $M_v(t)$ can be expressed as

$$M_u(t)=A_{M_u}\int_0^t\left\{-\ddot{u}_g(\tau)\right\}g_u(t-\tau)\mathrm{d}\tau, \tag{10}$$

$$M_v(t)=A_{M_v}\int_0^t\left\{-\ddot{v}_g(\tau)\right\}g_v(t-\tau)\mathrm{d}\tau. \tag{11}$$

STOCHASTIC RESPONSE IN FREQUENCY DOMAIN

The bending moment at the beam-end under the respective input of HVGM is expressed by the sum of responses to each direction as below:

$$f(t)=M_u(t)+M_v(t). \tag{12}$$

The auto-correlation function of $f(t)$ can be expressed as

$$\begin{aligned}E\left[f(t_1)f(t_2)\right]=&E\left[M_u(t_1)M_u(t_2)\right]+E\left[M_u(t_1)M_v(t_2)\right]\\&+E\left[M_v(t_1)M_u(t_2)\right]+E\left[M_v(t_1)M_v(t_2)\right],\end{aligned} \tag{13}$$

where $E[\ ]$ denotes the ensemble mean. Eq.(13) consists of four terms in time domain. These terms will be evaluated in detail later.

The auto-correlation function of the bending moment due to the horizontal input, i.e., the first term in Eq.(13), can be formulated in frequency domain by Fujita *et al*.(2008a)

$$E\left[M_u(t)^2\right]=A_{M_u}{}^2\int_{-\infty}^{\infty}\left[B_{\mathrm{c}}(t;\omega)^2+B_{\mathrm{s}}(t;\omega)^2\right]S_{uu}(\omega)\,\mathrm{d}\omega, \tag{14}$$

where subscriptions c and s mean cosine and sine terms in equations, and

$$B_{\mathrm{c}}(t;\omega)=\int_0^t c_u(\tau)g_u(t-\tau)\cos(\omega\tau)\mathrm{d}\tau, \tag{15}$$

$$B_{\mathrm{s}}(t;\omega)=\int_0^t c_u(\tau)g_u(t-\tau)\sin(\omega\tau)\mathrm{d}\tau. \tag{16}$$

The auto-correlation function of the bending moment due to the vertical input, i.e., the fourth term in Eq.(13), can be expressed as follows by the same procedure developed for the first term:

$$E\left[M_v(t)^2\right]=A_{M_u}^2\int_{-\infty}^{\infty}\left[C_{\mathrm{c}}(t;\omega)^2+C_{\mathrm{s}}(t;\omega)^2\right]S_{vv}(\omega)\,\mathrm{d}\omega, \tag{17}$$

where

$$C_{\mathrm{c}}(t;\omega)=\int_0^t c_v(\tau)g_v(t-\tau)\cos(\omega\tau)\mathrm{d}\tau, \tag{18}$$

$$C_{\mathrm{s}}(t;\omega)=\int_0^t c_v(\tau)g_v(t-\tau)\sin(\omega\tau)\mathrm{d}\tau. \tag{19}$$

The cross-correlation function of the bending moment due to HVGM can be formulated by some manipulations. The cross-correlation function of the functions $w_u(t)$ and $w_v(t)$ can be expressed in terms of the cross PSD function $S_{uv}(\omega)$ described by

$$E\left[w_u(\tau_1)w_v(\tau_2)\right]=\int_{-\infty}^{\infty}\left\{C_{uv}(\omega)+\mathrm{i}Q_{uv}(\omega)\right\}\mathrm{e}^{\mathrm{i}\omega(\tau_1-\tau_2)}\mathrm{d}\omega, \tag{20}$$

where $C_{uv}(\omega)$ and $Q_{uv}(\omega)$ are the real part (co-spectrum) and imaginary part (quad-spectrum) of $S_{uv}(\omega)$, respectively (Nigam, 1981). Substituting Eq.(20) into the cross-correlation function in frequency domain, the cross term, i.e., the sum of the second and third terms in Eq.(13), can be written as

$$\begin{aligned}&E\left[M_u(t)M_v(t)\right]+E\left[M_v(t)M_u(t)\right]\\&=2A_{M_u}A_{M_v}\int_{-\infty}^{\infty}\left\{f_1(t;\omega)C_{uv}(\omega)+f_2(t;\omega)Q_{uv}(\omega)\right\}\mathrm{d}\omega,\end{aligned} \tag{21}$$

where

$$f_1(t;\omega)=B_{\mathrm{c}}(t;\omega)C_{\mathrm{c}}(t;\omega)+B_{\mathrm{s}}(t;\omega)C_{\mathrm{s}}(t;\omega), \tag{22a}$$

$$f_2(t;\omega)=B_{\mathrm{c}}(t;\omega)C_{\mathrm{c}}(t;\omega)-B_{\mathrm{s}}(t;\omega)C_{\mathrm{s}}(t;\omega). \tag{22b}$$

Finally, the mean-squares of the sum of bending moments at beam-end may be expressed as

$$E[\{M_u(t)+M_v(t)\}^2]$$
$$=A_{M_u}^2\int_{-\infty}^{\infty}\{B_c(t;\omega)^2+B_s(t;\omega)^2\}S_{uu}(\omega)\mathrm{d}\omega$$
$$+2A_{M_u}A_{M_v}\int_{-\infty}^{\infty}\{f_1(t;\omega)C_{uv}(\omega)+f_2(t;\omega)Q_{uv}(\omega)\}\mathrm{d}\omega$$
$$+A_{M_v}^2\int_{-\infty}^{\infty}\{C_c(t;\omega)^2+C_s(t;\omega)^2\}S_{vv}(\omega)\mathrm{d}\omega. \quad (23)$$

CRITICAL EXCITATION METHOD FOR WORST CROSS PSD FUNCTION OF HVGM

The critical excitation problem may be stated as: Find the cross PSD function $S_{12}(\omega)=C_{12}(\omega)+\mathrm{i}Q_{12}(\omega)$ of HVGM so as to achieve $\max\limits_{S_{uv}(\omega)}\max\limits_{t}E[\{M_u(t)+M_v(t)\}^2]$.

When t is fixed and ω is specified, the transfer functions $f_1(t;\omega)$ and $f_2(t;\omega)$ defined in Eq.(22) can be regarded as pre-determined coefficients, not functions of t and ω. Therefore, the integrand in the second term of Eq.(23) can be regarded as the function $z(C_{uv}, Q_{uv})$ of C_{uv} and Q_{uv}:

$$f_1(t;\omega)C_{uv}(\omega)+f_2(t;\omega)Q_{uv}(\omega)=z(C_{uv},Q_{uv}). \quad (24)$$

Fig.5 illustrates the structure of the critical excitation problem. The critical excitation problem is to maximize the function $z(C_{uv}, Q_{uv})$ under the constraint $C_{uv}^2+Q_{uv}^2=S_{uu}(\omega)S_{vv}(\omega)$. This constraint corresponds to the assumption of the existence of a fully correlated multi-component ground input. The critical co-spectrum and quad-spectrum can then be obtained analytically as (Fujita *et al*., 2008a; 2008b)

$$C_{uv}(\omega)=f_1(t;\omega)\frac{\sqrt{S_{uu}(\omega)S_{vv}(\omega)}}{\sqrt{f_1(t;\omega)^2+f_2(t;\omega)^2}}, \quad (25)$$

$$Q_{uv}(\omega)=f_2(t;\omega)\frac{\sqrt{S_{uu}(\omega)S_{vv}(\omega)}}{\sqrt{f_1(t;\omega)^2+f_2(t;\omega)^2}}. \quad (26)$$

Fig.6 indicates the solution algorithm. By substituting Eqs.(25) and (26) into Eq.(21), Eq.(21) can be rewritten as the worst cross term maximizing the response quantity.

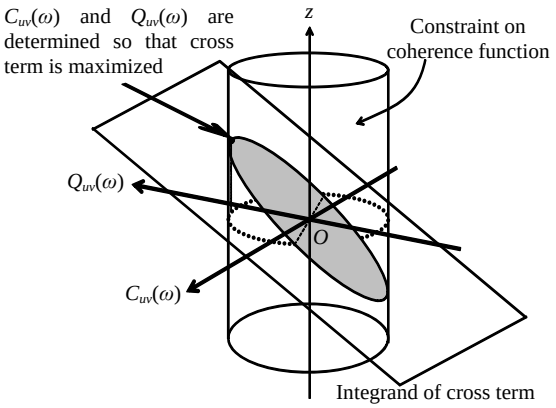

Fig.5 Structure of the critical excitation problem

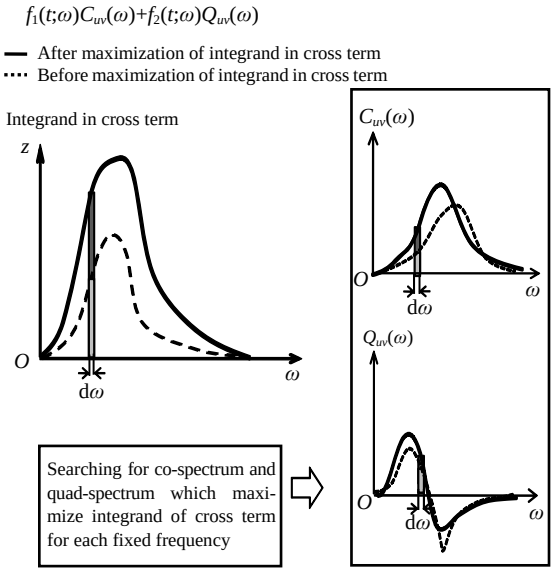

Fig.6 Solution algorithm of the critical excitation problem

$$E\left[M_u(t)M_v(t)\right]+E\left[M_v(t)M_u(t)\right]$$
$$=2A_{M_u}A_{M_v} \quad (27)$$
$$\times\int_{-\infty}^{\infty}\sqrt{f_1(t;\omega)^2+f_2(t;\omega)^2}\sqrt{S_{uu}(\omega)S_{vv}(\omega)}\mathrm{d}\omega.$$

Finally, Eq.(27) gives the closed-form worst cross term. In the integrand of Eq.(27), it can be observed that the property (transfer function $\sqrt{f_1(t;\omega)^2+f_2(t;\omega)^2}$) of a structure and that $\sqrt{S_{uu}(\omega)S_{vv}(\omega)}$ of ground motions are given separately. It can be understood that the relation between $S_{uu}(\omega)$ and $S_{vv}(\omega)$ is the key factor for the criticality (Fig.7).

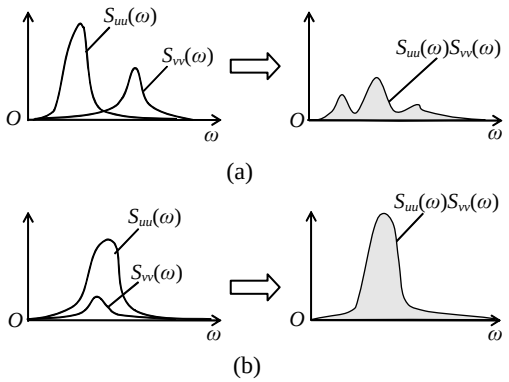

Fig.7 Relationship between horizontal and vertical PSD functions with regard to the response increase effect caused by correlation. (a) Weak correlation; (b) Strong correlation

CLOSED-FORM EXPRESSION OF THE WORST COMBINATION OF PSD FUNCTIONS

It can also be observed from Eq.(27) that the increase of response due to the correlation between multi-component ground motions from the square root of the sum of the squares (SRSS) response is indirectly related with the integration $\int_{-\infty}^{\infty}\sqrt{S_{uu}(\omega)S_{vv}(\omega)}\mathrm{d}\omega$ of geometric mean of both auto PSD functions. Under the constraint that the properties (shape) of respective auto PSD functions of ground motions are given (e.g., through the square of the velocity design spectrum (Fujita *et al*., 2008a; 2008b)), the critical correlation in Eq.(27) can be calculated based on the properties of a structure. However, since there may exist uncertainties with respect to the auto PSD functions of ground motions, it does not seem enough to consider the critical excitation problem under the constraint mentioned above. For this reason, let us find the worst combination of auto PSD functions which maximize the structural response under the constraint that the powers (areas) of the auto PSD functions are constant.

Iyengar and Manohar (1987) expressed the square root of the PSD function of the excitation in terms of linear combination of orthonormal function and determine their coefficients through eigenvalue analysis. Takewaki (2001) introduces a more simple probabilistic approach to define the PSD function as a band limited white noise (rectangle one). In the problem for one-directional input, the critical PSD function can be given by the resonant band limited white noise, not the velocity design spectrum, under the constraint that the area of the PSD function and the upper bound of the PSD function are given (Fig.8). In this paper, the central circular frequencies of the PSD functions of HVGM are assumed to be given by the resonant ones.

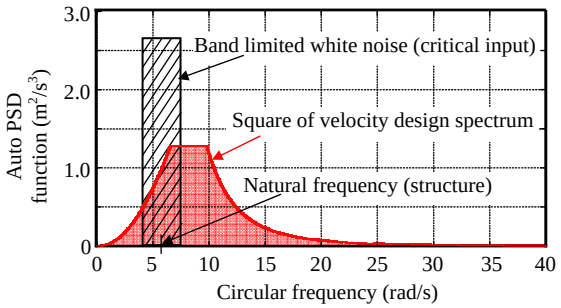

Fig.8 Relationship between auto PSD functions (band limited white noise and design spectrum)

As a constraint on the excitations, the following ones are introduced:

$$\int_{-\infty}^{\infty}S_{uu}(\omega)\mathrm{d}\omega\le\bar{S}_u, \tag{28a}$$

$$\int_{-\infty}^{\infty}S_{vv}(\omega)\mathrm{d}\omega\le\bar{S}_v. \tag{28b}$$

The values of $\bar{S}_u$ and $\bar{S}_v$ should be given appropriately according to the analysis of the auto PSD functions of recorded earthquake ground motions.

When ω_u, ω_v denote the fundamental natural circular frequencies in the horizontal and vertical directions of the structure and Ω_U, Ω_V express halves of the band widths of the auto PSD functions in the horizontal and vertical directions (Fig.9), the term $\int_{-\infty}^{\infty}\sqrt{S_{uu}(\omega)S_{vv}(\omega)}\mathrm{d}\omega$ can be expressed as

$$\begin{aligned}&\int_{-\infty}^{\infty}\sqrt{S_{uu}(\omega)S_{vv}(\omega)}\mathrm{d}\omega\\&=\sqrt{\frac{\alpha}{\Omega_U\Omega_V}}\bar{S}_u\{(\Omega_U+\Omega_V)/2-|\omega_u-\omega_v|\},\end{aligned} \tag{29}$$

where $\alpha=\bar{S}_v/\bar{S}_u$. In Eq.(29), it has been assumed that the central frequency of the auto PSD function coincides with the natural frequency of the structural model in both directions. The stationary point of Eq.(29) with respect to Ω_U, Ω_V can be derived by differentiating Eq.(29) with respect to Ω_U, Ω_V. The solution can be obtained as

$$\Omega_U = \Omega_V = 2\left|\omega_u - \omega_v\right|. \quad (30)$$

Eq.(30) implies that, if ω_u=ω_v, Ω_U=Ω_V=0 rad/s. This indicates that the worst input is the Dirac delta function in each direction in this model. However, it should be noted that the simplification from Eq.(27) into Eq.(29) is approximate and a fairly large error may arise depending on the model.

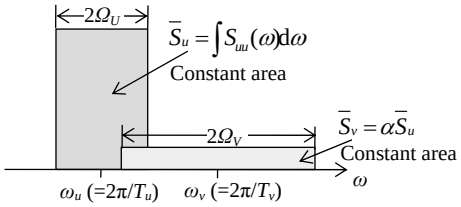

Fig.9 Variable PSD functions in respective directions

NUMERICAL ANALYSIS

The structural model analyzed in this section is shown in Fig.10. Two models with the span lengths L=17 m and 24 m are treated. The given geometrical and structural parameters are shown in Tables 2 and 3. Fig.11 illustrates the transfer functions $\sqrt{f_1(t;\omega)^2 + f_2(t;\omega)^2}$ for these two models. It can be observed that, while a simple and clear peak exists in the model of L=17 m due to the coincidence of both natural frequencies, a complex form arises in the model of L=24 m due to the non-coincidence of both natural frequencies. Table 1 shows the values of $\bar{S}_u$ and $\bar{S}_v$ for the above mentioned recorded ground motions. The maximum value of $\bar{S}_u$ is less than 9.0 m^2·rad/s^4. Based on this analysis, $\bar{S}_u$ and $\bar{S}_v$ are given by 10.0 and 2.5 m^2·rad/s^4.

Fig.12 compares the RMS of the bending moment due to the critical combination of multi-input with that due to the SRSS response without correlation terms. Fig.12a is drawn for the model of L=17 m and Fig.12b for that of L=24 m. These figures are plotted with respect to Ω_V for the fixed horizontal input circular frequency Ω_U=5 rad/s. It can be observed that, in the model of L=24 m, the difference between the bending moment due to the critical combination of multi-input and that due to the SRSS response is very small, while that is fairly large in the model of L=17 m.

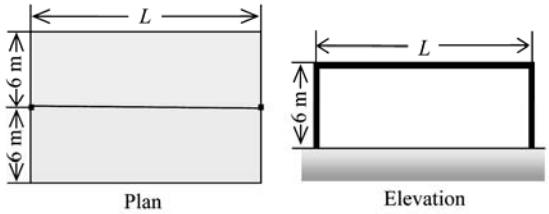

Fig.10 One-storey one-span moment resisting frame

Table 2 Structural member properties

Property	Value	
	Column	Beam
Cross-section (mm)	1000 ×1000×30*	1200 ×600×40×32**
Cross-sectional area (mm^2)	1.16×10^5	8.38×10^4
Second moment of area (mm^4)	1.83×10^{10}	1.99×10^{10}
Mass per unit length (kg/m)	912	657

* The height and width are 1000 mm, and the thickness is 30 mm; ** The height is 1200 mm, the width is 600 mm, the flange thickness is 40 mm, and the web thickness is 32 mm

Table 3 Geometrical and structural parameters

Parameter	Value	
	L=17 m	L=24 m
Horizontal stiffness (N/mm)	2.18×10^8	1.95×10^8
Vertical stiffness (N/mm)	1.07×10^8	4.16×10^7
Mass in horizontal direction (kg)	1.79×10^6	2.70×10^6
Mass in vertical direction (kg)	0.89×10^6	1.35×10^6
Horizontal natural period (s)	0.569	0.741
Vertical natural period (s)	0.572	1.131

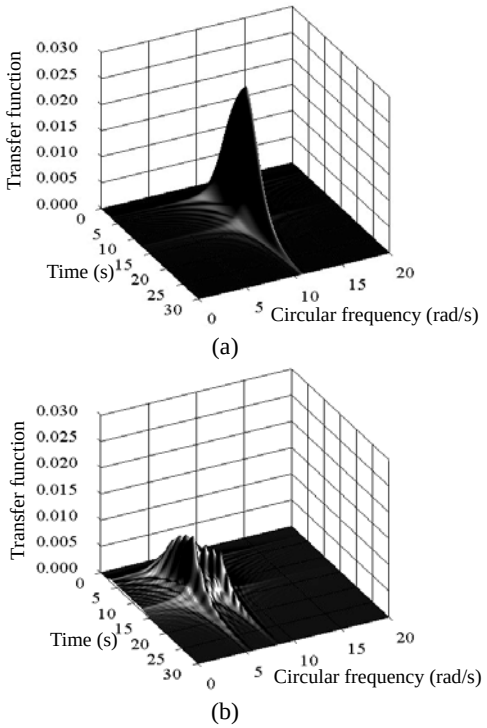

Fig.11 Transfer function $\sqrt{f_1(t;\omega)^2 + f_2(t;\omega)^2}$. (a) L=17 m; (b) L=24 m

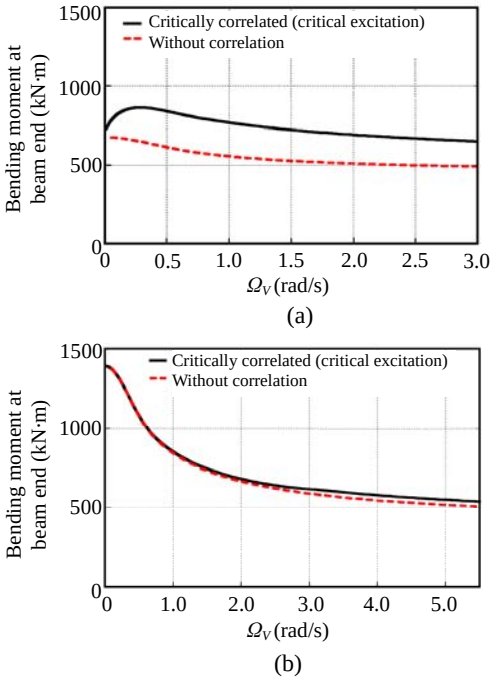

Fig.12 Comparison of the RMS bending moment to critically correlated multi-input with that to multi-input without correlation. (a) L=17 m; (b) L=24 m

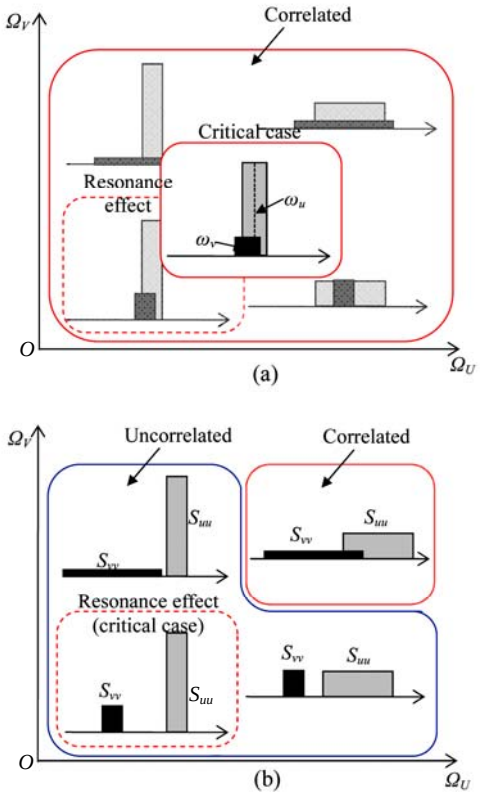

Fig.13 Critical combination of auto PSD functions of HVGM. (a) L=17 m; (b) L=24 m

According to Eq.(30), the stationary value of Ω_V is about 0.1 rad/s in the model of L=17 m. However, Fig.12 indicates that the maximum correlation term occurs around 0.2~0.5 rad/s. This may result from the approximation employed in the derivation of Eqs.(29) and (30). On the other hand, the stationary value of Ω_V is about 5.8 rad/s in the model of L=24 m. This corresponds fairly well with Fig.12b.

In the case of narrow band of Ω_U and Ω_V, the bending moment tends to be increased by the resonance effect. In addition, the bending moment can also be increased by the input correlation effect. Taking into account these two effects, the occurrence possibility of the worst combination of auto PSD functions can be investigated for each structural model (Fig.13). Fig.13a for the model of L=17 m indicates that the close location of natural frequencies in the horizontal and vertical directions causes the critical combination of auto PSD functions of HVGM as the largely overlapped shape. On the other hand, Fig.13b for the model of L=24 m illustrates that the separated location of natural frequencies in the horizontal and vertical directions provides the critical combination of auto PSD functions of HVGM as the un-overlapped shape.

Figs.14(a-1) and 14(a-2) show the 3D comparison of the RMS of the bending moment to the critically correlated multi-input with that to the multi-input without correlation for the model of L=17 m with respect to Ω_U and Ω_V. On the other hand, Figs.14(b-1) and 14(b-2) illustrate the corresponding comparison for the model of L=24 m. It is found that, while the model of L=17 m exhibits a remarkable difference between both cases, the model of L=24 m indicates a similar property between both cases. The influence of the band-widths of the auto PSD functions on the critical response can be observed clearly from these 3D figures.

Fig.15 illustrates the quantity of Eq.(27) for the critically correlated multi-input with respect to Ω_U and Ω_V for the models of L=17 m and 24 m. While the fundamental natural frequency of the model in the horizontal direction is almost equal to that in the vertical direction in the model of L=17 m, both are different in the model of L=24 m. These characteristics may cause the difference in Fig.15.

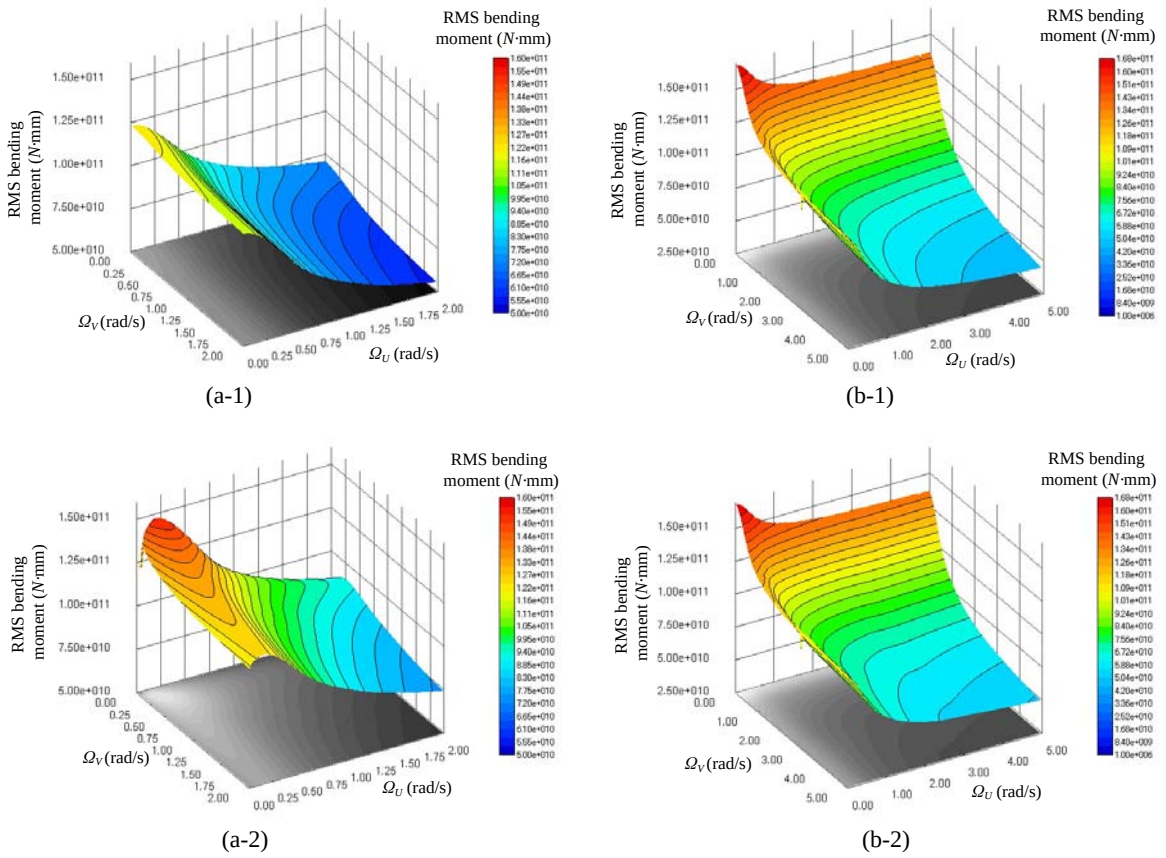

Fig.14 3D comparison of the root-mean-square (RMS) bending moment to critically correlated multi-input with that to multi-input without correlation. (a-1) and (b-1) without correlation (L=17 m and L=24 m); (a-2) and (b-2) critically correlated (L=17 m and L=24 m)

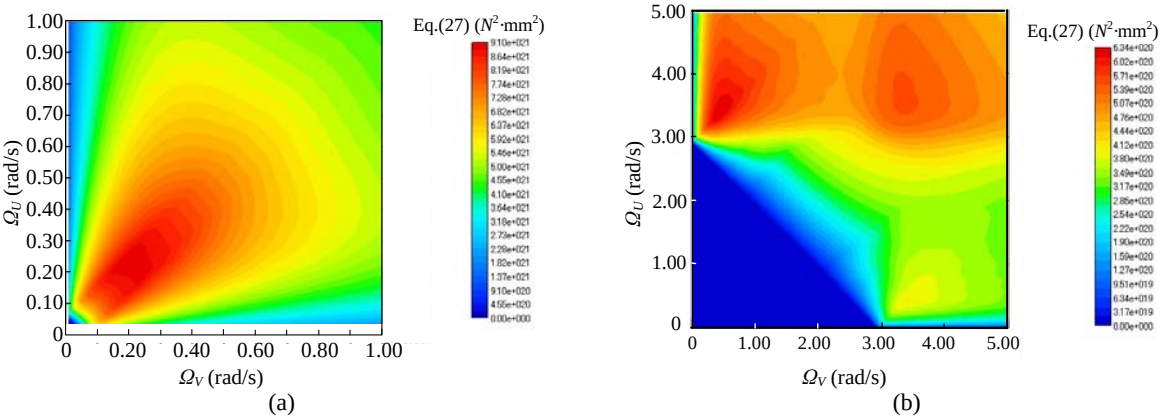

Fig.15 Quantity of Eq.(27) for critically correlated multi-input with respect to Ω_U and Ω_V. (a) L=17 m; (b) L=24 m

CONCLUSION

A new stochastic model of multi-component ground motion has been proposed in which the critical cross PSD function between the HVGM can be directly treated in the feasible complex plane. The following conclusions have been derived:

1. A critical excitation problem has been formulated for a moment-resisting frame subjected to HVGM. These multi-component ground motions are

characterized by a non-stationary stochastic model consisting of a given deterministic envelope function and a stochastic zero-mean Gaussian process.

2. The mean-squares bending moment at the beam-end has been shown to be the sum of the independent term due to each of HVGM and that due to their correlation. Each term has been formulated in the frequency domain. In the cross term of HVGM, the real part (co-spectrum) and imaginary part (quad-spectrum) of the cross PSD function can be regarded as independent variables. Since the auto PSD functions of HVGM are given and prescribed, the maximization in the critical excitation problem means the maximization of their correlation term.

3. The co-spectrum and quad-spectrum of the worst cross PSD function can be obtained by a devised algorithm including the interchange of the double maximization procedure in the time and cross PSD function domains. These expressions and the corresponding critical response have been described in closed form.

4. A closed-form expression of the critical relation of the auto PSD functions of simultaneous inputs has been derived in association with the relation with the horizontal and vertical structural properties.

5. Numerical examples indicate that the proposed algorithm can work very well. The RMS of the bending moment at the beam-end to the critical combination of the HVGM can become fairly larger than that by the SRSS estimate depending on the relation of the auto PSD functions of simultaneous inputs with the horizontal and vertical structural properties. The overlapping area of the auto PSD functions of HVGM in the frequency domain directly influences the critical cross PSD function between HVGM. These investigations have been made possible via the closed-form solutions stated above.

6. The coherence function between the HVGM of recorded earthquakes has been calculated and compared with the assumption introduced here. The coherence and cross PSD functions strongly depend on the type of earthquake ground motions and its portion. The prediction of coherence before their occurrence seems quite difficult. The critical excitation method will provide a meaningful insight even in these circumstances.

For simple and clear presentation of the essence of the formulation, a simple SDOF system has been treated in this paper. The extension of the present formulation to multi-degree-of-freedom (MDOF) or continuum models with finite-element discretization will be conducted in the future.

References

Abbas, A.M., Manohar, C.S., 2002a. Critical spatially varying earthquake load models for extended structures. *Journal of Structural Engineering*, **29**(1):39-52.

Abbas, A.M., Manohar, C.S., 2002b. Investigating into critical earthquake load models within deterministic and probabilistic frameworks. *Earthquake Engineering & Structural Dynamics*, **31**(4):813-832. [doi:10.1002/eqe.124]

Abbas, A.M., Manohar, C.S., 2007. Reliability-based vector nonstationary random critical earthquake excitations for parametrically excited systems. *Structural Safety*, **29**(1):32-48. [doi:10.1016/j.strusafe.2005.11.003]

Abbas, A.M., Takewaki, I., 2009. The use of probabilistic and deterministic measures to identify unfavorable earthquake records. *Journal of Zhejiang University SCIENCE A*, **10**(5):619-634. [doi:10.1631/jzus.A0930001]

Drenick, R.F., 1970. Model-free design of aseismic structures. *Journal of the Engineering Mechanics Division, ASCE*, **96**(EM4):483-493.

Fujita, K., Takewaki, I., Nakamura, N., 2008a. Critical disturbance for stress resultant in long-span moment-resisting frames subjected to horizontal and vertical simultaneous ground inputs. *Journal of Structural and Construction Engineering (Transactions of AIJ)*, **73**(626):551-558 (in Japanese). [doi:10.3130/aijs.73.551]

Fujita, K., Yoshitomi, S., Tsuji, M., Takewaki, I., 2008b. Critical cross-correlation function of horizontal and vertical ground motions for uplift of rigid block. *Engineering Structures*, **30**(5):1199-1213. [doi:10.1016/j.engstruct.2007.07.017]

Iyengar, R.N., Manohar, C.S., 1987. Nonstationary random critical seismic excitations. *Journal of Engineering Mechanics*, **113**(4):529-541. [doi:10.1061/(ASCE)0733-9399(1987)113:4(529)]

Japanese Geotechnical Society, 1996. Special issue on geotechnical aspects of the January 17 1995 Hyogoken-Nambu Earthquake. *Soils and Foundations*, special issue.

Manohar, C.S., Sarkar, A., 1995. Critical earthquake input power spectral density function models for engineering structures. *Earthquake Engineering & Structural Dynamics*, **24**(12):1549-1566. [doi:10.1002/eqe.4290241202]

Nigam, N.C., 1981. Introduction to Random Vibrations. MIT Press, p.76.

Sarkar, A., Manohar, C.S., 1996. Critical cross power spectral density functions and the highest response of multi-supported structures subjected to multi-component earthquake excitations. *Earthquake Engineering & Structural Dynamics*, **25**(3):303-315. [doi:10.1002/(SICI)1096-9845(199603)25:3<303::AID-EQE559>3.0.CO;2-P]

Sarkar, A., Manohar, C.S., 1998. Critical seismic vector random excitations for multiply supported structures. *Journal of Sound and Vibration*, **212**(3):525-546. [doi:10.1006/jsvi.1997.1460]

Smeby, W., Der Kiureghian, A., 1985. Modal combination rules for multicomponent earthquake excitation. *Earthquake Engineering & Structural Dynamics*, **13**(1):1-12. [doi:10.1002/eqe.4290130103]

Strasser, F.O., Bommer, J.J., 2009. Large-amplitude ground-motion recordings and their interpretations. *Soil Dynamics and Earthquake Engineering*, **29**(10):1305-1329. [doi:10.1016/j.soildyn.2009.04.001]

Takewaki, I., 2001. A new method for nonstationary random critical excitation. *Earthquake Engineering & Structural Dynamics*, **30**(4):519-535. [doi:10.1002/eqe.21]

Takewaki, I., 2002. Seismic critical excitation method for robust design: A review. *Journal of Structural Engineering, ASCE*, **128**(5):665-672. [doi:10.1061/(ASCE)0733-9445(2002)128:5(665)]

Takewaki, I., 2004a. Critical envelope functions for non-stationary random earthquake input. *Computers & Structures*, **82**(20-21):1671-1683. [doi:10.1016/j.compstruc.2004.04.004]

Takewaki, I., 2004b. Bound of earthquake input energy. *Journal of Structural Engineering, ASCE*, **130**(9):1289-1297.

Takewaki, I., 2006a. Probabilistic critical excitation method for earthquake energy input rate. *Journal of Engineering Mechanics*, **132**(9):990-1000.

Takewaki, I., 2006b. Critical Excitation Methods in Earthquake Engineering. Elsevier Science, Oxford.